



TECHNICAL ARTICLE

Column Separation of Vanadium(V) from Complex Sulfuric Solution Using Trialkylamine-Impregnated Resins

BO CHEN,¹ SHENXU BAO ^{1,2,5} and YIMIN ZHANG^{1,2,3,4}

1.—School of Resources and Environmental Engineering, Wuhan University of Technology, Wuhan 430070, People's Republic of China. 2.—Hubei Key Laboratory of Mineral Resources Processing and Environment, Wuhan 430070, People's Republic of China. 3.—State Environmental Protection Key Laboratory of Mineral Metallurgical Resources Utilization and Pollution Control, Wuhan University of Science and Technology, Wuhan 430081, Hubei Province, People's Republic of China. 4.—Hubei Collaborative Innovation Center for High Efficient Utilization of Vanadium Resources, Wuhan University of Science and Technology, Wuhan 430081, Hubei Province, People's Republic of China. 5.—e-mail: sxbao@whut.edu.cn

Separation of V(V) from simulated complex vanadium-bearing (SCV) solution containing Al(III), Fe(III), P(V), and Si(IV) using trialkylamine (N235)-impregnated resins has been investigated. Batch experiments proved that the optimal pH for adsorption and separation of V(V) from impurities was 1.8. Column experiments showed that V(V) was well adsorbed and separated from the impurities under conditions of flow rate of 1.0 mL min⁻¹ and bed height of 12 cm. Most of the impurities that adsorbed on the N235-impregnated resin were effectively eluted with only 2.92% loss of V(V) using 12 bed volumes (BV) of 2 wt.% Na₂SO₄. Afterwards, V(V) was concentrated about 3.4 times and most of it was recovered using cycle desorption with 1 BV of 14 wt.% Na₂CO₃. The concentration of the impurities in the initial feed solution was greatly decreased using the present method, implying that V(V) can be effectively separated from SCV solution by such column operations.

INTRODUCTION

Vanadium, as a significant strategic resource for modern industry, is extensively used in steel, aerospace, and chemical industries due to its unique properties, such as hardness, tensile strength, and fatigue resistance.¹ Extraction of vanadium from low-grade vanadium resources, such as vanadium-bearing shale, spent catalyst, and vanadiferous slag, is attracting increasing attention worldwide.² Currently, the technique of acid leaching with H₂SO₄ for vanadium extraction from these low-grade vanadium resources is widely used due to its high vanadium recovery and low energy consumption,³ but many impurities, such as Al(III), Fe(III), P(V), and Si(IV), are also leached together with vanadium, making it more difficult to separate and recover vanadium from the resulting acid leaching solution.^{4,5} Therefore, separation and recovery of vanadium from the complex acid leaching solutions is a key and essential process for vanadium extraction.

Generally, solvent extraction (SX) and ion exchange (IX) are adopted to separate and recover vanadium from the acid leaching solution. In the SX process, bis(2-ethylhexyl)phosphoric acid (D2EHPA) is widely used for recovery of vanadium.^{4,6} However, D2EHPA offers poor selectivity for V(IV) from solutions containing Fe(III). Trialkylamine (N235) has also been applied to separate vanadium from acid leaching solution by many researchers due to its distinctive selectivity for vanadium.^{7,8} Meanwhile SX commonly suffers from problems including loss of extractants, complicated processes, and difficult phase separation due to emulsification.⁹ IX is an attractive alternative separation method because of its intrinsic properties, including easy operation, lack of pollution, and low cost, but it also generally suffers from the disadvantages of relatively low selectivity for metals.^{10,11} Various kinds of techniques have been applied to remove impurity ions prior to IX to address this disadvantage, including crystallization or precipitation methods. However, neutralization of the leaching solution to precipitate Fe(III) leads to not only

high alkali consumption but also substantial loss of vanadium, while crystallization processes generally require high operating temperatures above 95°C.¹⁰ To overcome these problems, use of solvent-impregnated resins (SIRs) prepared by incorporating extractants into a macroporous polymer has been proposed for separation and recovery of metals from aqueous solution. These materials are widely used in different fields because of their advantages for both SX and IX.^{12–14} Tang et al.¹⁵ prepared D2EHPA-impregnated resins and found that the SIRs exhibited high adsorption capacity for V(IV). Liang et al.¹⁶ investigated the separation and recovery of V(IV) from sulfuric solutions containing Fe(III) and Al(III) using D2EHPA-impregnated resins, revealing that the SIRs achieved poor separation of V(IV) and Al(III). In the above-mentioned approach for separation of V(IV) using D2EHPA-impregnated resins, the SIRs present poor selectivity but high adsorption capacity for V(IV). Thus, it is necessary to increase the selectivity of SIRs while retaining their high adsorption capacity for vanadium. Based on the high efficiency of N235 in solvent extraction of vanadium, we prepared N235-impregnated resins and used them to separate V(V) from sulfuric solution in our previous work.¹⁷ The results showed that the SIRs offered high performance for adsorption of V(V). However, most research on SIRs has focused on separation and recovery of metal ions from simple solution systems,^{14,15,17–19} while literature on complicated ions systems is limited. To achieve high selectivity when separating vanadium from complex acid leaching solution and promote the application of SIRs on an industrial scale using fixed columns, in the present study, N235-impregnated resins were used to separate and purify V(V) from simulated complex vanadium-bearing (SCV) solution containing V(V), Al(III), Fe(III), P(V), and Si(IV) by column separation. The operation parameters of the packed column, such as the flow rate, bed height, and initial V(V) concentration, were investigated to determine the optimal column conditions to achieve high adsorption and separation performance for V(V) from impurities, and the stepwise desorption process for impurities and V(V) from the loaded SIRs was studied to achieve effective separation and purification efficiency of V(V) from the impurities. This aim of this work is to obtain pure vanadium-rich solution for vanadium precipitation, for example, by hydrothermal hydrogen reduction.²⁰ Furthermore, this study may promote the development and application of SIRs in the fields of separation and purification of metals from complex aqueous solution.

EXPERIMENTAL PROCEDURES

Materials

Trialkylamine (N235, R₃N, R = C₈–C₁₀) purchased from Qinshi Technology Co., Ltd., China

was used as extractant. Petroleum ether with boiling point range of 60°C to 90°C was used to dilute N235.

Amberlite® XAD-16HP macroporous resin supplied by Shanghai Anland Co., Ltd., China was used as the support for the SIRs. Resin with size of 0.425 mm to 0.850 mm was selected by screening to prepare SIRs. The resins were pretreated before use as follows: First, the resins were soaked in ethanol for 4 h to remove remaining monomers and other types of impurity due to the fabrication process, followed by washing with deionized water until the effluent was clear, and then filtered and dried at 60°C in a vacuum oven for 12 h.

Based on actual vanadium-bearing acid leaching solution,²¹ SCV solution was prepared by three steps. Firstly, pure V(V) solution was prepared by dissolving a certain amount of V₂O₅ in dilute sulfuric solution (pH 0.8). Secondly, the pH of the pure V(V) solution was adjusted to about 1.6 using concentrated sodium hydroxide. Finally, certain amounts of Al₂(SO₄)₃·18H₂O, Fe₂(SO₄)₃·9H₂O, Na₃PO₄·12H₂O, and Na₂SiO₃·9H₂O (purchased from Sinopharm Chemical Reagent Co., Ltd., China) were added into the pure V(V) solution, then the mixture was filtrated after the solution became clear. The pH of the filtrate was then adjusted to 1.8 using concentrated sulfuric acid. In the whole study except for “Effects of Initial V(V) Concentration” section on the effects of the initial V(V) concentration, the concentration of vanadium was about 1200 mg L⁻¹ while the content of Al(III), Fe(III), P(V), and Si(IV) was about 8600 mg L⁻¹, 2025 mg L⁻¹, 360 mg L⁻¹, and 120 mg L⁻¹, respectively. In the work described in “Effects of Initial V(V) Concentration” section, the concentration of vanadium was varied from 400 mg L⁻¹ to 1200 mg L⁻¹ while keeping the concentrations of impurity ions constant as shown above. All of these chemical reagents were of analytical grade.

Preparation of SIRs

N235 (12 mL) was firstly diluted in 18 mL petroleum ether, then the diluted N235 was mixed with the pretreated XAD-16HP resins (at liquid-to-solid ratio of 30:1 mL g⁻¹). Subsequently, the mixtures were subjected to ultrasound (CP505, Vernon Hills, IL) under conditions of power of 100 W, irradiation time of 5 min, and extractant concentration of 40 vol.%. After impregnation, the resins were separated using a Buchner funnel then washed with deionized water until the effluent was clear. Finally, the obtained N235-impregnated resins were heated at 60°C in a vacuum oven for 12 h to remove remaining diluent prior to use. Detailed information on the prepared N235-impregnated resins is presented in our previous work.¹⁷

Batch Adsorption Experiments

Batch adsorption experiments were conducted by adding 1.0 g SIR to 40 mL SCV solution at various

initial pH values ranging from 0.6 to 2.0. After the mixtures had been shaken for 14 h to reach adsorption equilibrium in a bath oscillator (SHA-2, Jintan Yitong Electronic Co., Ltd., China) at 25°C, the solutions were filtrated and the concentrations of V(V), Al(III), Fe(III), P(V), and Si(IV) were determined by inductively coupled plasma atomic emission spectrometry (ICP-AES, Optima4300DV; PerkinElmer, USA). The adsorption capacity of each SIR for metal ions, Q_M (mg g⁻¹), was calculated using Eq. 1:

$$Q_M = \frac{(C_0 - C_e)V}{m_2}, \quad (1)$$

where V is the volume of SCV solution (L), C_0 and C_e are the initial and equilibrium concentrations of metal ions in solution (mg L⁻¹), respectively, and m_2 is the weight of the dry SIR (g).

Packed Column Experiments

A quartz glass tube with inner diameter of 10 mm and length of 300 mm was used in the packed column experiments. The wall effect in the packed column operation process can be ignored due to the fact that the inner diameter of the column was about 12 times larger than that of the resin particles.²²

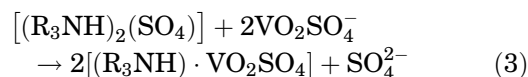
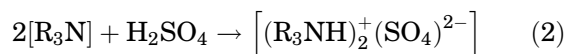
In the column operation model, a certain amount of dry SIR was added into the column, then the packed-bed column was pretreated with dilute H₂SO₄ until the pH of the effluent was the same as that of the feed SCV solution, which was adjusted to the optimal value according to the batch adsorption experiments. Adsorption experiments were performed at room temperature by pumping the SCV solution at a certain flow rate through the packed column using a peristaltic pump (BT100-1F, Longer, China). Effluent samples were collected at 1-bed-volume (BV) intervals to analyze the concentrations of the studied metal ions. The adsorption processes were stopped when the concentrations of the metal ions in the effluent reached 90% of those in feed solution, which is referred to as the saturation point. The effects of different flow rates (0.5 mL min⁻¹, 1.0 mL min⁻¹, and 1.5 mL min⁻¹), SIR bed height (H) in the column (4 cm, 8 cm, and 12 cm), and initial V(V) concentration (400 mg L⁻¹, 800 mg L⁻¹, and 1200 mg L⁻¹) were investigated based on the shape of the breakthrough curve and the breakthrough volume, both of which are predominant factors for determining the operation and dynamic response of an adsorption column.¹⁶ The breakthrough point is defined as the point at which the concentrations of metal ions in the effluent (C) reaches about 50% of those in the feed solution.²³ The breakthrough volume is defined as the volume of solution that has been fed by the breakthrough point, which can be used to compare the adsorption and separation performance of the packed SIR column for V(V) and impurity ions.

RESULTS AND DISCUSSION

Effects of pH

The effects of pH on the adsorption of V(V) and the impurities from the SCV solution onto the SIRs in batch adsorption experiments are shown in Fig. 1.

It can be seen that the pH had a significant influence on the adsorption of V(V) onto the SIRs. The adsorption percentage of V(V) onto the SIRs improved from 2.54% to 92.89% as the pH was increased from 0.6 to 2.0 (Fig. 1). It is widely accepted that the mechanism of absorption of metal ions onto SIRs is identical to that of ions extracted by an impregnated extractant in solvent extraction.²⁴ N235 can extract the anionic form of V(V) through ion exchange in liquid-liquid extraction systems according to the following reactions:^{25,26}



The species distribution of V(V) in solution was obtained using Medusa software and is shown in Supplementary Fig. S-1 (Electronic Supplementary Material).²⁷ As shown in Fig. S-1, V(V) exists predominantly in the form of VO₂⁺ and VO₂SO₄⁻ in solution at lower pH, but the percentage of the anionic form of V(V), VO₂SO₄⁻, increases at higher pH, so more anionic V(V) can react with N235 via reaction (3). Hence, the adsorption percentage of V(V) on the SIRs increased with increasing pH (Fig. 1).

The adsorption percentage of Fe(III) on the SIRs fluctuated from 4.44% to 6.67% mg g⁻¹ over the studied pH range, which can be attributed to the fact that Fe(III) can partially form anionic Fe(SO₄)₂⁻

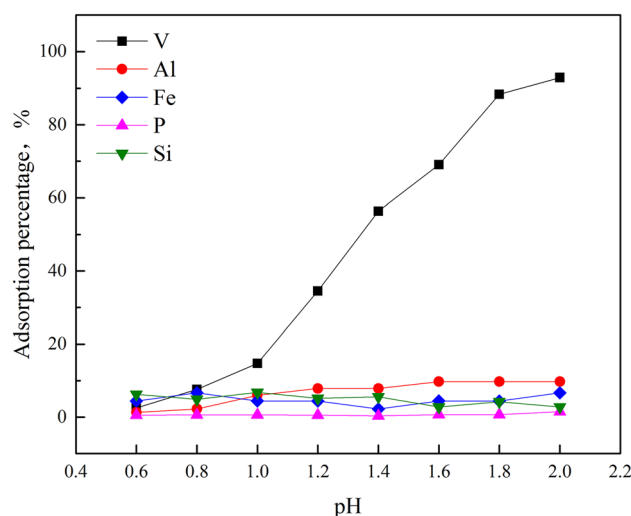
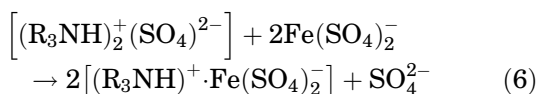
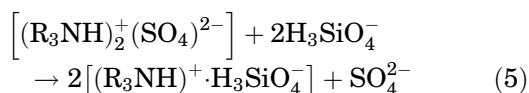
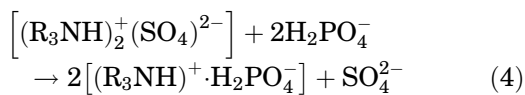


Fig. 1. Effects of pH on adsorption percentage of V(V) and impurities; $C_0(V) = 1200$ mg L⁻¹, adsorption time 14 h, 25°C.

by combining with SO_4^{2-} in sulfuric solution.²⁸ Moreover, small amounts of P(V) and Si(IV) were absorbed from the solutions, which can be attributed to the fact that P(V) is present as neutral H_3PO_4 and H_2PO_4^- while Si(IV) is present as neutral H_4SiO_4 and anionic H_3SiO_4^- in acidic solution (pH 0 to 4).⁸ The anions H_2PO_4^- , H_3SiO_4^- , and $\text{Fe}(\text{SO}_4)_2^-$ could be adsorbed onto the N235 impregnated in the resins through ion exchange as shown in Eqs. 4 to 6.



The adsorption characteristics of the impurity ions except for Al(III) onto the SIRs are approximately consistent with those of the common meals extracted by N235.⁸ The species distribution of Al(III) in solution is shown in supplementary Fig. S-2, revealing that Al(III) bonds with SO_4^{2-} to form anionic $\text{Al}(\text{SO}_4)_2^-$, the fraction of which increased with increasing pH from 0 to 2 (Supplementary Fig. S-2). Thus, the adsorption percentage of Al(III) onto the SIRs increased with increasing pH (Fig. 1).

During the adsorption process, the adsorption percentages of Al(III) and Fe(III) were much higher than those of P(V) and Si(IV), which can be attributed to the relatively higher contents of the former in the SCV solution. Thus, Al(III) and Fe(III) might interfere with the adsorption of V(V) due to their relatively larger loading, while P(V) and Si(IV) exerted little influence on it within the pH range of 0.6 to 1.8. When the initial pH exceeded 1.8, precipitation of Fe(III) became noticeable in the adsorption process. Therefore, the optimal initial pH was selected as 1.8 for the following column adsorption experiments.

Column Adsorption

Effects of Flow Rate

The breakthrough curves showing C/C_0 versus the volume of feed solution are shown in Fig. 2 for flow rates of 0.5 mL min^{-1} , 1.0 mL min^{-1} , and 1.5 mL min^{-1} .

As can be seen from Fig. 2, the breakthrough curves for V(V) showed an initial rapid increase and then gradually approached equilibrium. This type of breakthrough curve was also reported by Brunson and Sabatini²⁹ for fluoride removal using aluminum-coated wood and bone char, being attributed

to significant intraparticle diffusion restriction. The total quantity of adsorbed V(V), the treated volume, and the V(V) removal percentage at the breakthrough and saturation points for each flow rate are presented in Supplementary Table S-1.

As is evident from these results, the breakthrough and saturation volumes for V(V) decreased with increasing flow rate, implying that increasing the flow rate reduced the volume of treated solution efficiently until breakthrough, thereby decreasing the operation time of the SIR column bed.⁹ Accordingly, the adsorption capacity of the SIR beds for V(V) also declined with increasing flow rate. This can be attributed to the fact that the residence time of V(V) within the bed declines with increase of the flow rate. If the residence time of the metal ions in the column is not long enough at a given flow rate, the ions will leave the column early before reaching adsorption equilibrium.³⁰ The saturation adsorption capacities for these impurities evaluated from the sorption data are presented in Supplementary Table S-2.

These results show that more impurities could be adsorbed onto the SIRs at lower flow rates, especially for V(V) (Supplementary Table S-2). This can be ascribed to the fact that the solute can react with the SIR more sufficiently when their contact time is long enough at lower flow rates, and the adsorption capacity of the SIRs for the impurities is increased as well. Thus, considering both the adsorption and separation characteristics of V(V) and impurities, the optimal flow rate for subsequent experiments was determined to be 1.0 mL min^{-1} .

Effects of Bed Height

The breakthrough curves for the adsorption of V(V) and the impurities when using a bed height of 4 cm, 8 cm, and 12 cm are shown in Fig. 3.

As shown in Fig. 3, the breakthrough and saturation volumes of V(V) varied with the SIR bed height. The adsorption capacity and removal percentage of V(V) for the SIRs at the breakthrough and saturation points are presented in Supplementary Table S-3.

It is obvious from these results that the breakthrough and saturation volumes increased with increasing SIR bed height. Meanwhile, the difference between the breakthrough curves of impurities and V(V) also increased with increasing SIR bed height, implying that the separation of V(V) from the impurities was more effective at greater fixed bed height, probably due to the increased mass of SIR, providing more sorption sites and longer contact time for absorption of metal ions.^{16,31} In addition, Fig. 3 shows that the metal ions had more time to diffuse into the SIR particles and interact with the extractant loaded in the pores as the bed height was increased.³² The adsorption capacities of the SIRs for the studied impurities are presented in Supplementary Table S-4.

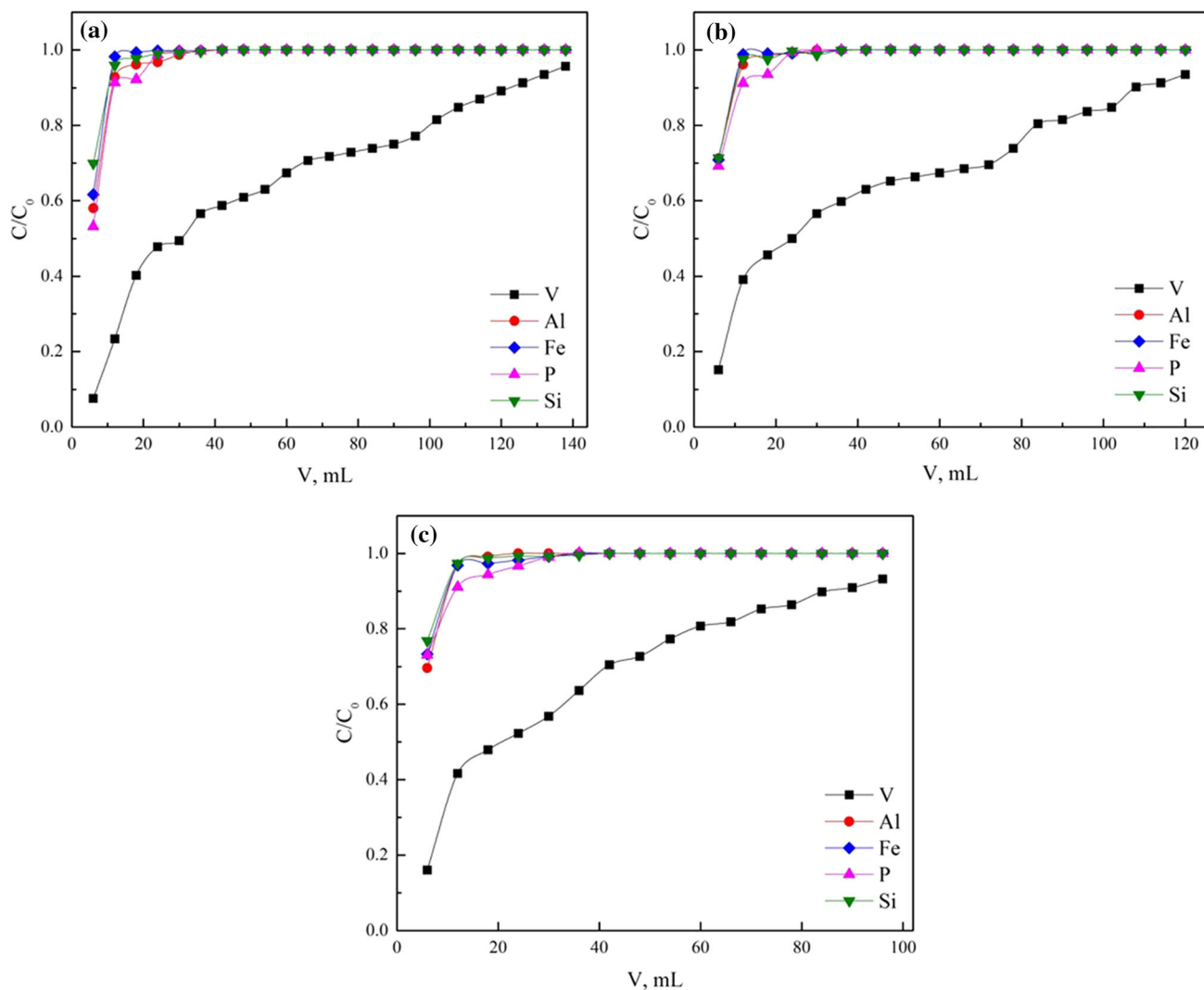


Fig. 2. Breakthrough curves of V(V) and impurities at different flow rates: (a) 0.5 mL min^{-1} , (b) 1.0 mL min^{-1} , and (c) 1.5 mL min^{-1} ; pH 1.8, $H = 8 \text{ cm}$, $C_0(\text{V}) = 1200 \text{ mg L}^{-1}$.

The adsorption capacity of the SIRs for the impurities decreased with increasing SIR bed height, which can probably be attributed to the lower affinity towards the impurities compared with V(V), and the replacement of the adsorbed impurities by V(V). Based on these results, the optimal column bed height for subsequent adsorption experiments was determined to be 12 cm.

Effects of Initial V(V) Concentration

Figure 4 shows the breakthrough curves for the adsorption of V(V) and the impurities onto the SIRs at different initial V(V) concentrations with constant concentrations of impurities. As illustrated in Fig. 4, the initial V(V) concentration had a significant impact on the breakthrough curves. The parameters obtained from the breakthrough curves are summarized in Supplementary Tables S-5 and S-6. The compositions of the feed solutions with

different initial vanadium concentrations are presented in Supplementary Table S-7.

It is obvious that the breakthrough and saturation points for V(V) occurred earlier at higher V(V) concentrations, and accordingly the steepness (dC/dt) of the breakthrough curves was higher in comparison with those obtained at lower V(V) concentration, indicating improved performance of the SIR bed at higher V(V) concentration.³³ However, the quantities of treated solution and V(V) adsorbed on the resin at the breakthrough and saturation points were higher at lower V(V) concentration, since the lower concentration gradient resulted in slower transport due to the decrease of the diffusion coefficient.³⁴

These results verify that the use of a higher initial V(V) concentration can improve the adsorption rate by the packed column but decrease the adsorption capacity of the SIRs for V(V). Thus, the adsorption capacity of the SIRs for V(V) at the breakthrough

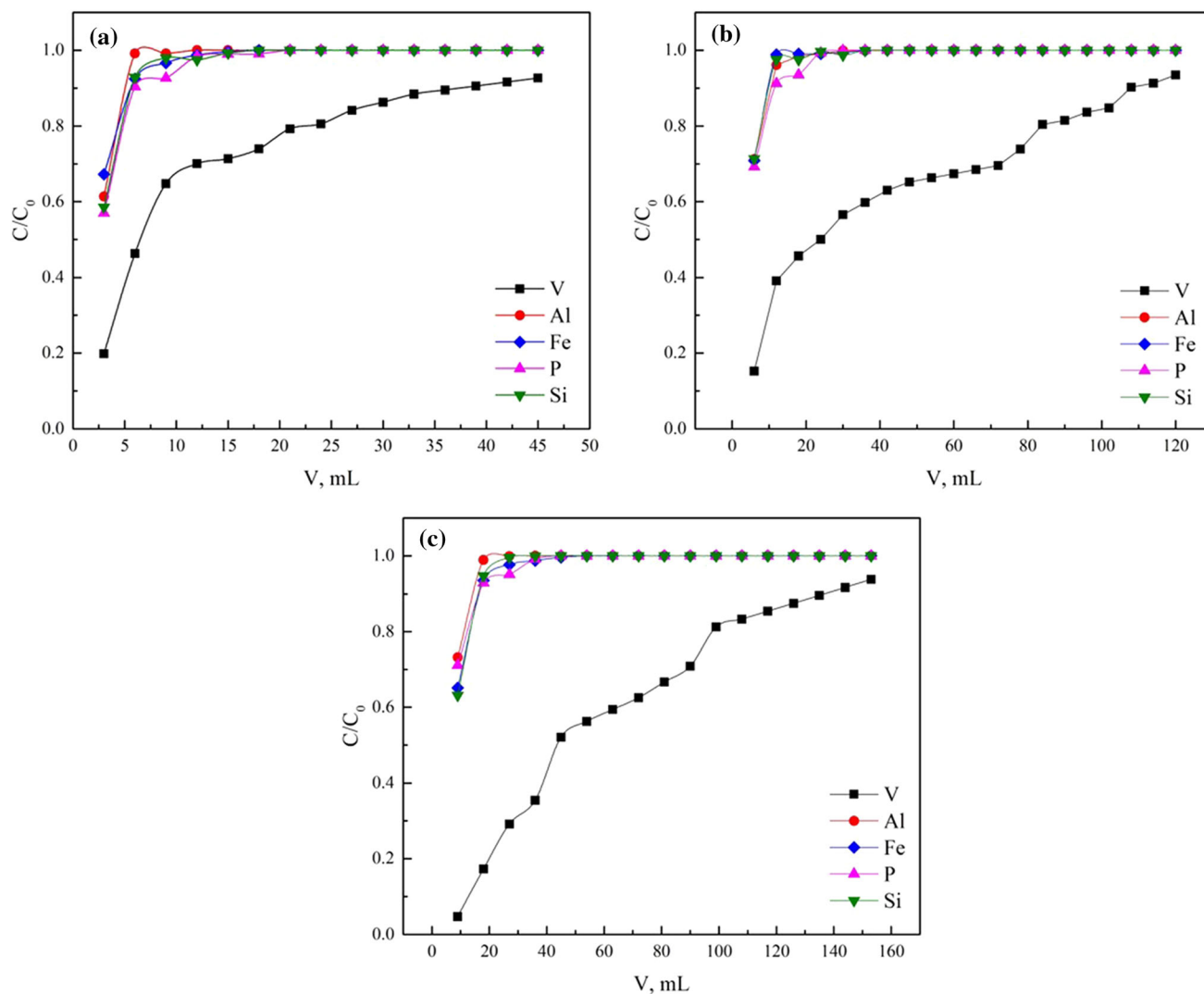


Fig. 3. Breakthrough curves of V(V) and impurities for different SIR bed heights: (a) 4 cm, (b) 8 cm, and (c) 12; pH 1.8, flow rate 1.0 mL min^{-1} , $C_0(\text{V}) = 1200 \text{ mg L}^{-1}$.

and saturation points were lower at higher V(V) concentration, even though the driving force for V(V) adsorption was stronger in this condition.

Elution of Vanadium from the Loaded SIRs

Column adsorption experiments were conducted at conditions of flow rate of 1.0 mL min^{-1} , bed height of 12 cm, and initial V(V) concentration of 1200 mg L^{-1} . When the adsorption process was completed, the loaded SIRs containing vanadium and impurities were eluted to remove impurities, then stripped using Na_2CO_3 solution to recover V(V).

Effects of Eluting Agents on Removal of Impurities

The loaded SIRs were eluted using 2 wt.% Na_2SO_4 or 2 wt.% HCl at fixed liquid-to-solid ratio of 10:1. As shown in Fig. S-3, compared with 2 wt.% HCl, which just offered the advantage of eluting

P(V), 2 wt.% Na_2SO_4 could effectively elute Al(III), Fe(III), and Si(IV) but less V(V). Thus, considering the eluting percentage of the impurities and the loss of V(V), 2 wt.% Na_2SO_4 was appropriate for the eluting procedure.

Effects of Eluent Volume on Removal of Impurities

Figure 5 reveals that the eluting percentage of the impurities increased with increasing volume of Na_2SO_4 . These results show that most of the loaded P(V), Al(III), and Si(IV) could be effectively eluted from the loaded resins, while the eluting percentage of Fe(III) was about 63.76% and only a small amount of vanadium (about 3.04%) was eluted from the resins when using 13 BV (117 mL) of Na_2SO_4 . The difference between the eluting behavior of vanadium versus the impurities indicates that V(V) can be effectively separated from Al(III), Fe(III), P(V), and Si(IV) using such an elution procedure. Very small amounts of the impurities

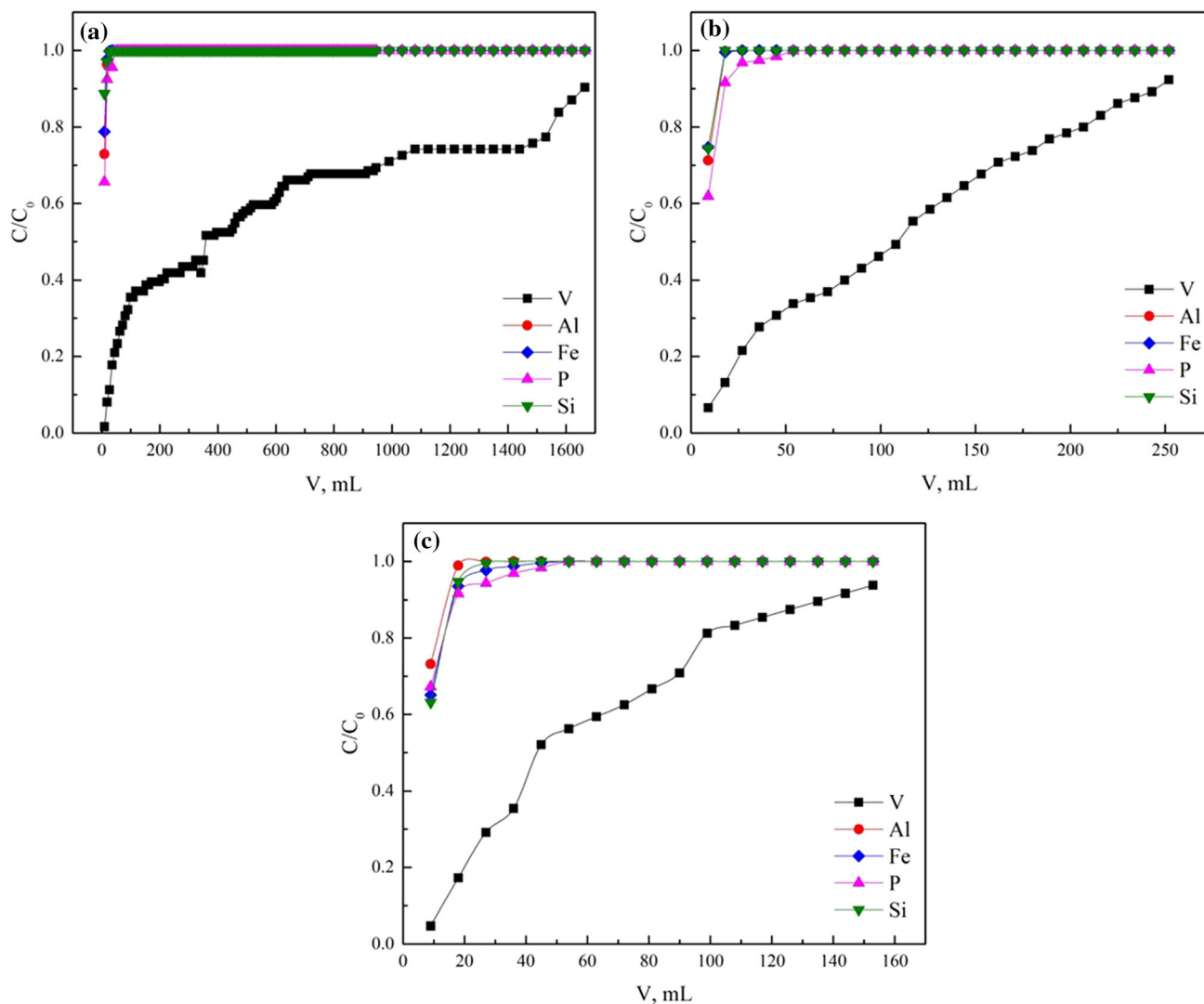


Fig. 4. Breakthrough curves for adsorption of V(V) from impurities at different initial V(V) concentrations: (a) 400 mg L⁻¹, (b) 800 mg L⁻¹, and (c) 1200 mg L⁻¹; pH 1.8, flow rate 1.0 mL min⁻¹, $H = 12$ cm.

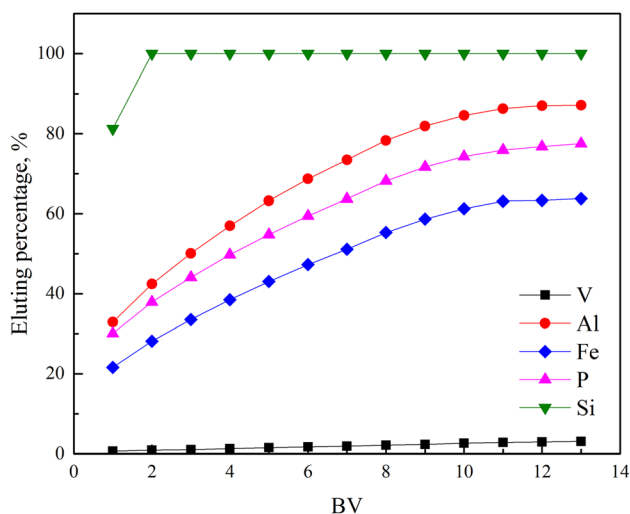
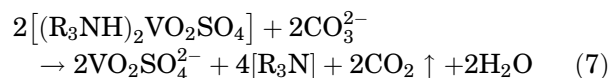


Fig. 5. Effect of eluent volume on eluted percentage of vanadium and impurities.

remained on the SIRs, which may not affect the stripping of vanadium. When the Na_2SO_4 volume was increased to 12 BV (108 mL), the eluting percentage of the impurities approached the balance (Fig. 5). No significant difference was observed in the eluting percentage of impurities when the Na_2SO_4 volume was increased above 12 BV. Therefore, 12 BV was selected as the optimal Na_2SO_4 volume for the eluting procedure.

Effects of Na_2CO_3 Concentration

During extraction of V(V) using N235, Na_2CO_3 is commonly adopted to strip V(V). The reaction underlying this mechanism can be expressed as⁷



The eluted SIRs were stripped using Na_2CO_3 of different concentrations under conditions of liquid-

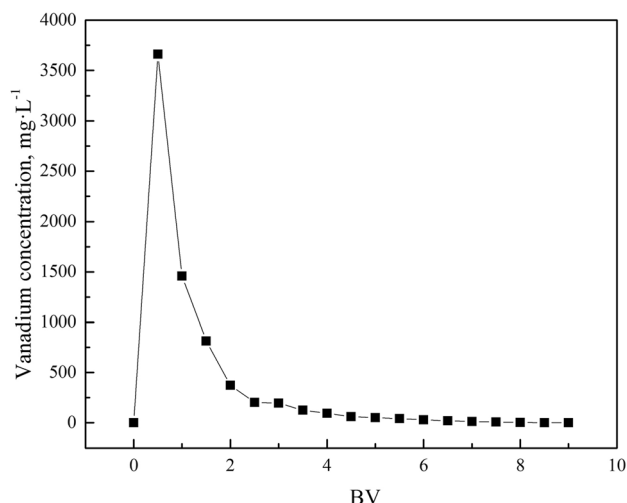


Fig. 6. Stepwise elution curves of V(V).

to-solid ratio of 5:1 and constant flow rate of 1.0 mL min^{-1} . The results showed that the stripping percentage of V(V) increased from 48.54% to 87.31% as the Na_2CO_3 concentration was increased from 2% to 18%, which can be attributed to the increase in the CO_3^{2-} concentration (Supplementary Fig. S-4). Considering the small differences in the stripping percentage of V(V) when the Na_2CO_3 concentration was increased from 14% to 18%, 14% Na_2CO_3 was chosen as the optimal solution for elution of V(V) in subsequent experiments.

Effects of Na_2CO_3 Volume

Figure 6 clearly reveals that the maximum concentration of V(V) in the stripped solution ($3661.85 \text{ mg L}^{-1}$) was obtained when using 0.5 BV Na_2CO_3 . The concentration of V(V) was less than 20 mg L^{-1} when the volume of Na_2CO_3 used was greater than 6.5 BV. It is obvious that most of the V(V) could be stripped when 0.5 to 1.5 BV Na_2CO_3 was used, indicating that the stripping efficiency of V(V) was extremely low when the volume of Na_2CO_3 was greater than 1.5 BV. Thus, the method of cyclic desorption by using 1 BV Na_2CO_3 was applied to increase the V(V) enrichment ratio and stripping efficiency. The concentration of V(V) in the stripped solution after different numbers of cycles is shown in Supplementary Fig. S-5.

Supplementary Fig. S-5 reveals that the V(V) concentration and enrichment ratio obviously increased with increasing numbers of desorption cycles from one to four, suggesting that such a cyclic desorption method can indeed improve the stripping efficiency and achieve a high enrichment ratio of V(V). Increasing the number of cycles from four to six led to a decrease in the vanadium concentration in the stripped solution, which can be ascribed to readsorption of V(V) onto the SIRs. Thus, four was selected as the optimal number of desorption cycles.

Table I. Composition of solutions for each step of column separation process (mg L^{-1})

Element	V	Al	Fe	P	Si
Feed solution	1187	8600	2034	352.8	131.4
Adsorbed solution	800.2	8394	1977	344.9	130.2
Eluent solution	14.35	226.8	46.81	7.76	1.33
Stripped solution	4069	9.19	17.16	7.61	1.80

Table II. Concentration ratio of V(V) and impurities in feed and stripped solutions

Concentration ratio	V/Al	V/Fe	V/P	V/Si
Feed solution	0.14	0.58	3.36	9.03
Stripped solutions	443	238	535	2262

Mass Balance in Column Separation Process

A designed flowchart for the separation and recovery of V(V) using the SIRs in column mode is shown in Supplementary Fig. S-6, and the distribution of V(V), Al(III), Fe(III), P(V), and Si(IV) at each step of the column separation process is summarized in Table I.

As can be seen from this table, the concentration of V(V) in the eluted solution was $4068.72 \text{ mg L}^{-1}$, indicating a V(V) enrichment ratio of about 3.4 with most of the V(V) being recovered from the eluted SIRs. Meanwhile, the concentrations of Al(III), Fe(III), P(V), and Si(IV) were greatly reduced compared with those in the initial feed solution. The concentration ratio of V(V) to impurities in the feed and stripped solution is listed in Table II.

It is obvious that the concentration ratio of V(V) to impurities in the stripped solutions was significantly increased compared with that in the feed solution, implying that V(V) can be effectively separated from solutions containing Al(III), Fe(III), P(V), and Si(IV) by using N235-impregnated resins in column operation. The final vanadium-rich solution could be used as raw material for vanadium precipitation by the hydrothermal hydrogen reduction,²⁰ while the effluent after the column adsorption could be processed using continuous multicolumn SIRs or returned to the acid leaching process.

CONCLUSION

Batch and column adsorption experiments were carried out to verify the applicability of N235-impregnated resins for selective separation of V(V) from SCV solution. The optimal pH value for separation of V(V) from the complex solution was found to be 1.8. Specifically, use of a high initial V(V) concentration improved the adsorption rate but decreased the adsorption capacity of V(V)

through the packed SIR columns. Most of the impurities that adsorbed onto the loaded SIRs could be effectively eluted with loss of only 2.92% V(V) when using 2 wt.% Na₂SO₄ with a volume of 12 BV. V(V) was concentrated about 3.4 times, and most of it was recovered from the eluted SIRs, when using the method of cycle desorption with 1 BV of 14 wt.% Na₂CO₃. Furthermore, the concentration ratio of V(V) to impurities in the stripped solutions was significantly increased compared with that in the feed solution, implying that V(V) can be effectively separated from SCV solution by column operation. The results of this study demonstrate that N235-impregnated resins may represent an alternative method for separation of V(V) from complex acid leaching solutions and could also be applied for separation and purification of other high-concentration metals from aqueous solution.

ACKNOWLEDGEMENTS

This research was supported by National Natural Science Foundation of China (51874222, 51404177), and the Major Technical Innovation Project of Hubei Province (2018ACA157).

CONFLICT OF INTEREST

There are no conflicts to declare.

ELECTRONIC SUPPLEMENTARY MATERIAL

The online version of this article (<https://doi.org/10.1007/s11837-019-03944-4>) contains supplementary material, which is available to authorized users.

REFERENCES

1. R.R. Moskalyk and A.M. Alfantazi, *Miner. Eng.* 16, 793 (2003).
2. Y.M. Zhang, S.X. Bao, T. Liu, T.J. Chen, and J. Huang, *Hydrometallurgy* 109, 116 (2011).
3. M.T. Li, C. Wei, S. Qiu, X.J. Zhou, C.X. Li, and Z.G. Deng, *Hydrometallurgy* 104, 193 (2010).
4. X.B. Li, C. Wei, Z.G. Deng, M.T. Li, C.X. Li, and G. Fan, *Hydrometallurgy* 105, 359 (2011).
5. Y.Z. Yuan, Y.M. Zhang, T. Liu, T.J. Chen, and J. Huang, *RSC Adv.* 7, 18438 (2017).
6. G. Hu, D. Chen, L. Wang, J.C. Liu, H. Zhao, Y. Liu, T. Qi, C. Zhang, and P. Yu, *Sep. Purif. Technol.* 125, 59 (2014).
7. A. Chagnes, C. Fosse, B. Courtaud, J. Thiry, and G. Cote, *Hydrometallurgy* 105, 328 (2011).
8. X. Yang, Y.M. Zhang, S.X. Bao, and C. Shen, *Sep. Purif. Technol.* 164, 49 (2016).
9. M.A.A. El-Ghaffar, Z.H. Abdel-Wahab, and K.Z. Elwakeel, *Hydrometallurgy* 96, 27 (2009).
10. W. Li, Y.M. Zhang, T. Liu, J. Huang, and Y. Wang, *Hydrometallurgy* 131–132, 1 (2013).
11. A.N. Nikoloski and K. Ang, *Extr. Metall. Rev.* 35, 369 (2014).
12. K.K. Yadav, D.K. Singh, M. Anitha, L. Varshney, and H. Singh, *Sep. Purif. Technol.* 118, 350 (2013).
13. J. Bokhove, T.J. Visser, B. Schuur, and A.B.D. Haan, *React. Funct. Polym.* 86, 67 (2015).
14. N.V. Nguyen, J.C. Lee, J. Jeong, and B.D. Pandey, *Chem. Eng. J.* 219, 174 (2013).
15. Y.P. Tang, S.X. Bao, Y.M. Zhang, and L. Liang, *React. Funct. Polym.* 113, 50 (2017).
16. L. Liang, S.X. Bao, Y.M. Zhang, and Y.P. Tang, *Chem. Eng. Res. Des.* 111, 109 (2016).
17. B. Chen, S.X. Bao, Y.M. Zhang, R.W. Zheng, and R. Soc, *Open. Sci.* 5, 171746 (2018).
18. S. Nishihama, K. Kohata, and K. Yoshizuka, *Sep. Purif. Technol.* 118, 511 (2013).
19. N. Kabay, M. Demircioğlu, H. Ekinci, M. Yüksel, M. Sağlam, and M. Streat, *React. Funct. Polym.* 38, 219 (1998).
20. G.B. Zhang, Y.M. Zhang, S.X. Bao, J. Huang, and L.H. Zhang, *Miner. Basel* 7, 182 (2017).
21. C. Shen, Y.M. Zhang, S.X. Bao, J. Huang, and X. Yang, *Chin. J. Rare. Met.* 41, 422 (2017).
22. L.C. Lin, J.K. Li, and R.S. Juang, *Desalination* 225, 249 (2008).
23. D. Saha, E.S. Vadivu, R. Kumar, and C.R.V. Subramani, *J. Radioanal. Nucl. Chem.* 298, 1309 (2013).
24. S.X. Bao, Y.P. Tang, Y.M. Zhang, and L. Liang, *Chem. Eng. Technol.* 39, 1377 (2016).
25. L. Zeng and C.Y. Cheng, *Hydrometallurgy* 98, 10 (2009).
26. J.R. Kumar, S.M. Shin, H.S. Yoon, C.W. Nam, K.W. Chung, J.Y. Lee, and T.P. Jin, *Sep. Purif. Technol.* 49, 819 (2014).
27. L. Puigdomenech, *Medusa Software* (Sweden: KTH University, 2015).
28. M.C. Martí-Calatayud, D.C. Buzzi, M. García-Gabaldón, E. Ortega, A.M. Bernardes, J.A.S. Tenório, and V. Pérez-Herranz, *Desalination* 343, 120 (2014).
29. L.R. Brunson and D.A. Sabatini, *Sci. Total Environ.* 580, 488 (2014).
30. E. Malkoc, Y. Nuhoglu, and Y. Abali, *Chem. Eng. J.* 119, 61 (2006).
31. M.F. Attallah, E.H. Borai, M.A. Hilal, F.A. Shehata, and M.M. Abo-Aly, *J. Hazard. Mater.* 195, 73 (2011).
32. D. Bulgariu and L. Bulgariu, *Bioresour. Technol.* 129, 374 (2013).
33. A. Singh, D. Kumar, and J.P. Gaur, *Water Res.* 46, 779 (2012).
34. Z. Aksu and F. Gönen, *Process Biochem.* 39, 599 (2004).

Publisher's Note Springer Nature remains neutral with regard to jurisdictional claims in published maps and institutional affiliations.